A Negative Result for a QATNU Spin-2 Search

Hardware controls, cube source-response checks, and a connected-correlator QMC falsifier

Joshua Farrow
Independent Research

June 2026

Status. This manuscript records a negative result. It does not establish spin-2 emergence, a graviton, a Ward identity, a dispersion relation, or a Mercury number. It reports that the tested small-graph hardware protocols and the tested diagonal bond-bond QMC mechanism do not provide evidence for a collective tensor mode.

Abstract

The QATNU/SRQID program asks whether a measurement-free bond-promotion mechanism can generate an emergent spin-2 channel rather than inserting one by assumption. This paper records a deliberately negative result from the first hardware-facing and QMC-facing tests of that idea. A hardware-readable qubit encoding was implemented with one matter qubit per graph vertex and one bond qubit per graph edge. Exact simulation, local Qiskit/Aer checks, and IBM Quantum runs were performed for Phase-0 negative controls, two-dimensional graph families, a 20-qubit $2 \times 2 \times 2$ cube, uniform and compact source-response circuits, and a full-ladder QMC mechanism scan on 2^3 and 3^3 open cubes.

The result is negative but useful. The Phase-0 and Phase-1 hardware circuits produce nonzero scalar and bond observables while remaining explicitly inadmissible for a spin-2 claim. The IBM Kingston cube source-response workflow runs end-to-end, but the uniform-source response changes sign between the deeper four-step circuit and the shallower two-step circuit, and the compact source remains boundary dominated. These hardware observations validate plumbing, not physics.

The decisive result comes from the QMC branch. A diagonal line-graph bond-bond coupling, $K_{\mathrm{bb}} = 0.02$, initially appeared promising because it increased the static tensor susceptibility per edge, especially on the 3^3 cube. However, the final connected-correlator diagnostic decomposes the susceptibility into diagonal single-edge variance and off-diagonal inter-edge covariance. At $\chi_{\max} = 10$, $\beta = 2$, and eight seeds, $K_{\mathrm{bb}} = 0.02$ raises χ_T/edge from 1.505861 to 3.698071 on the 3^3 cube, but the connected inter-edge contribution moves from -0.000483 to -1.685906 per edge. The increase is instead carried by single-edge variance, which rises to 5.383977 per edge. Therefore the tested mechanism produces local bond-ladder population variance, not a growing positive connected tensor correlator.

This rules out the present bond-bond mechanism as evidence for spin-2 emergence. It does not rule out the broader QATNU/SRQID program. It defines the next gate: future candidates must show positive connected inter-edge tensor covariance, stability under $\chi_{\max}$, and finite-size scaling before being promoted to hardware interpretation.

Contents

1 Question and claim boundary **2**

2 Hardware-readable model **2**

3 Phase-0 and Phase-1 hardware controls **3**

4 IBM Kingston cube source-response checks **3**

5 Full-ladder QMC mechanism scan **4**

6 Connected inter-edge falsifier **5**

7 What is ruled out **6**

8 What is not ruled out **6**

9 Reproducibility **6**

10 Conclusion **7**

1 Question and claim boundary

The practical question was not whether a small superconducting device could "discover gravity." The question was whether the QATNU/SRQID observable stack could pass a stricter early discipline:

> It should measure active scalar and bond dynamics, but it should refuse to interpret inadmissible geometries or local ladder fluctuations as spin-2 evidence.

This paper answers that question for the tested branch. The answer is negative for the spin-2 interpretation and positive for the diagnostic discipline. The work reported here rules out the current hardware/QMC evidence path:

- the small hardware graphs are useful controls but not spin-2 substrates;
- the IBM cube source-response circuits are executable but not physics-stable tensor measurements;
- the tested K_{bb} mechanism increases total tensor variance by increasing single-edge ladder variance rather than positive connected inter-edge correlation.

The result does not rule out all QATNU/SRQID models. It rules out a specific claim path: using the present small-graph circuits or the present diagonal bond-bond QMC mechanism as evidence for an emergent collective spin-2 channel.

2 Hardware-readable model

For a graph $G = (V, E)$, the hardware encoding assigns one matter qubit to every vertex and one bond qubit to every edge. This is the smallest bond-ladder truncation, equivalent to $\chi_{\max} = 2$ in the hardware circuits:

$$\mathcal{H}_{\mathrm{hw}} = \bigotimes_{i \in V} \mathbb{C}_i^2 \otimes \bigotimes_{e \in E} \mathbb{C}_e^2. \tag{1}$$

The Phase-0 Hamiltonian used for exact simulation and circuit generation was

$$H = H_{\mathrm{mat}} + H_{ZZ} + H_{\mathrm{bond}} + H_{\mathrm{prom}}, \tag{2}$$

with

$$H_{\mathrm{mat}} = \frac{\omega}{2} \sum_{i \in V} X_i, \tag{3}$$

$$H_{ZZ} = J_0 \sum_{\langle i,j \rangle \in E} Z_i Z_j, \tag{4}$$

$$H_{\mathrm{bond}} = \Delta_B \sum_{e \in E} n_e, \tag{5}$$

$$H_{\mathrm{prom}} = \lambda \sum_{e = \langle i,j \rangle} F_{ij} X_e, \tag{6}$$

where

$$n_e = \frac{I - Z_e}{2}, \qquad F_{ij} = \frac{1 - Z_i Z_j}{2}. \tag{7}$$

The scalar load used throughout the hardware checks is

$$\Lambda_i = \sum_{e \ni i} \log(1 + \langle n_e \rangle), \tag{8}$$

and the basic scalar-load spread is

$$\Delta\Lambda = \max_i \Lambda_i - \min_i \Lambda_i. \tag{9}$$

3 Phase-0 and Phase-1 hardware controls

The first requirement was that trivial or structurally inadmissible graphs must not pass. Four exact Phase-0 controls were tested: path, cycle, star, and diamond. All produced nonzero bond observables and all returned `FAIL_EXPECTED_NEGATIVE_CONTROL`.

Graph	Matter	Edges	Qubits	Mean bond occupation	Verdict
Path	4	3	7	0.128778	fail expected
Cycle	4	4	8	0.130146	fail expected
Star	4	3	7	0.130499	fail expected
Diamond	4	4	8	0.130146	fail expected

Table 1: Phase-0 exact negative controls. The scalar/bond sector is active, but the graphs are not spin-2 admissible.

The Phase-1 graph-family extension added small non-one-dimensional and two-dimensional fixtures. These were not promoted to spin-2 candidates. They were used to validate circuit generation, IBM submission, count extraction, and analysis on larger graph families.

Topology	Vertices	Edges	Qubits	Role	Verdict
House	5	6	11	small 2D motif	negative control
Square 2×3	6	7	13	2D pipeline	not spin-2 admissible
Triangular 2×3	6	9	15	2D pipeline	not spin-2 admissible
Square 3×3	9	12	21	scaling smoke	not spin-2 admissible
Triangular 3×3	9	16	25	scaling smoke	not spin-2 admissible

Table 2: Phase-1 hardware graph families. These circuits are useful for hardware plumbing and scalar/bond readout. They are not 3+1-dimensional infrared spin-2 tests.

The Kingston graph-family runs were executable up to 25 qubits. The strongest triangular-size hardware trend was an increase in scalar-load spread, but the analysis contained no tensor-channel observable, no layout-controlled repeat matrix sufficient for a physics claim, and no scalar/vector impostor rejection. Those runs therefore remain hardware validation, not evidence for spin-2 emergence.

4 IBM Kingston cube source-response checks

The next hardware step was a $2 \times 2 \times 2$ cube with 8 matter qubits and 12 bond qubits. The first Kingston package contained a baseline cube and a matched uniform x-axis source-response pair at 2000 shots. All three jobs completed on `ibm_kingston`.

The uniform-source response was

$$\Delta M_{xx} = M_{xx}(+J_x) - M_{xx}(-J_x) = -0.022667, \qquad \chi^{\text{source}}_{T,xx} = -0.226667. \tag{10}$$

Run	Backend	Job ID	Submitted UTC	Shots	Distinct bitstrings
Baseline cube	`ibm_kingston`	`d8dm8gtmdsks73d44g70`	2026-05-30 22:27	2000	1922
$+J_x$	`ibm_kingston`	`d8donca4gq0s73aqjlq0`	2026-05-31 01:15	2000	1938
$-J_x$	`ibm_kingston`	`d8dong24gq0s73aqjlug`	2026-05-31 01:15	2000	1919

Table 3: First Kingston $2 \times 2 \times 2$ cube package. The circuits ran, but the near-maximal bitstring spread and depth make the finite-difference response an engineering check rather than a physics measurement.

A shallower two-step Trotter version reduced the transpiled depth from 1671 to 813 and the CZ count from 942 to 411. Its source response changed sign:

$$\Delta M_{xx} = 0.027833, \qquad \chi_{T,xx}^{\text{source}} = 0.278333. \tag{11}$$

A compact source at amplitude 0.2 gave

$$\Delta M_{xx} = 0.030000, \qquad \chi_{T,xx}^{\text{source}} = 0.075000. \tag{12}$$

The sign and amplitude instability is the key hardware conclusion. The cube source-response machinery works end-to-end, but these circuits do not define a stable tensor susceptibility on present hardware. They are not negative evidence against the theory; they are negative evidence against interpreting this small, deep, noisy cube source protocol as spin-2 physics.

5 Full-ladder QMC mechanism scan

The QMC branch lifted the bond ladder beyond the one-qubit hardware truncation and tested a diagonal line-graph bond-bond coupling. The scan used open $2 \times 2 \times 2$ and $3 \times 3 \times 3$ cubes and a static tensor observable built from axis-aligned bond occupations.

For time-averaged tensor components $\bar{M}_a$, the static susceptibility was computed as

$$\chi_T = \beta \sum_a \left\langle (\bar{M}_a - \langle \bar{M}_a \rangle)^2 \right\rangle . \tag{13}$$

The reported intensive value is $\chi_T/|E|$.

Early scans showed that $K_{\text{bb}} = 0.02$ was the only mechanism worth checking further. At $\chi_{\max} = 8$, it raised $\chi_T/|E|$ on both L2 and L3, and at $\chi_{\max} = 10$, $\beta = 2$, it produced the strongest total response:

Topology	$\chi_{\max}$	K_{bb}	$\langle n \rangle$	$\chi_T/\lvert E\rvert$
2^3 cube	10	0.000	0.713375 ± 0.005259	1.500858 ± 0.023981
2^3 cube	10	0.020	0.967665 ± 0.037716	1.854037 ± 0.058112
3^3 cube	10	0.000	0.720107 ± 0.007726	1.505861 ± 0.051795
3^3 cube	10	0.020	2.707870 ± 0.216995	3.698071 ± 0.335568

Table 4: The narrow QMC candidate before connected-correlator subtraction. The total susceptibility increase looked interesting, especially on L3, but it coincided with a large bond-ladder occupation increase.

This table alone was not decisive. A local occupation fluctuation and a collective tensor correlation can both increase the total variance. The next diagnostic separated them.

6 Connected inter-edge falsifier

Let m_e be the imaginary-time averaged bond occupation on edge e for one QMC measurement. The tensor observable is linear in m_e:

$$\bar{M}_a = \sum_e W_{ae} m_e. \tag{14}$$

The total susceptibility can therefore be decomposed as

$$\chi_T = \beta \sum_{e,f} \left(W^T W\right)_{ef} \mathrm{Cov}(m_e, m_f). \tag{15}$$

The diagonal part,

$$\chi_T^{\mathrm{diag}} = \beta \sum_e \left(W^T W\right)_{ee} \mathrm{Var}(m_e), \tag{16}$$

is single-edge ladder variance. The off-diagonal part,

$$\chi_T^{\mathrm{conn}} = \beta \sum_{e \neq f} \left(W^T W\right)_{ef} \mathrm{Cov}(m_e, m_f), \tag{17}$$

is the connected inter-edge tensor covariance. A collective spin-2 candidate should not depend on the total variance rising while χ_T^{conn} is zero or negative.

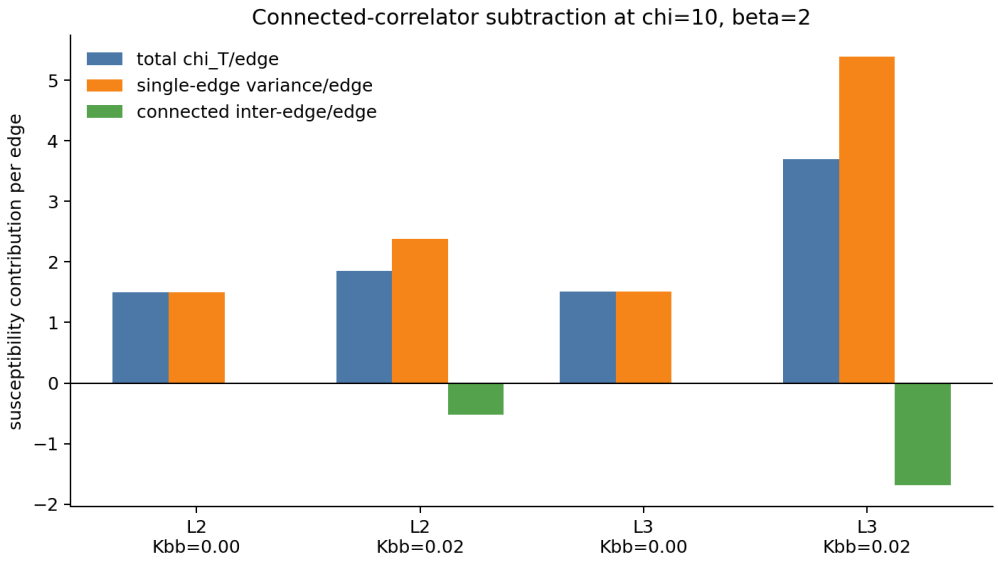

Figure 1: Final discriminating QMC diagnostic. The $K_{\mathrm{bb}} = 0.02$ runs increase the total susceptibility, but the connected inter-edge contribution becomes negative. The total increase is carried by diagonal single-edge variance.

The subtraction is decisive. On the 3^3 cube, turning on $K_{\mathrm{bb}} = 0.02$ changes

$$\Delta(\chi_T/|E|) = +2.192210, \tag{18}$$

$$\Delta(\chi_T^{\mathrm{diag}}/|E|) = +3.877632, \tag{19}$$

$$\Delta(\chi_T^{\mathrm{conn}}/|E|) = -1.685423. \tag{20}$$

The apparent tensor susceptibility is not an inter-edge collective correlation. It is local bond-ladder variance with an anticorrelated inter-edge subtraction.

Topology	K_{bb}	$\chi_T/\lvert E\rvert$	single-edge/edge	connected/edge	connected fraction
2^3 cube	0.000	1.500858	1.495647	0.005211	0.002948
2^3 cube	0.020	1.854037	2.379352	−0.525315	−0.280917
3^3 cube	0.000	1.505861	1.506344	−0.000483	−0.005969
3^3 cube	0.020	3.698071	5.383977	−1.685906	−0.526047

Table 5: Connected-correlator decomposition at $\chi_{\max} = 10$, $\beta = 2$, 12 time slices, 30 thermalization sweeps, 240 measurement sweeps, and eight seeds.

7 What is ruled out

The data rule out the following claim:

> The current small-graph hardware response or the tested diagonal bond-bond QMC mechanism provides evidence for an emergent spin-2 tensor sector.

More specifically:

1. Phase-0 and Phase-1 hardware circuits are useful negative controls and pipeline tests, but they are structurally inadmissible for 3+1-dimensional spin-2 emergence.
2. The 2^3 IBM cube source-response protocol is executable, but the response is not stable under shallower circuit design and source localization.
3. The QMC $K_{\mathrm{bb}} = 0.02$ mechanism raises total tensor variance by increasing single-edge ladder variance, not by generating positive connected inter-edge tensor covariance.

This is not merely an absence of a positive result. It is an active falsifier for this mechanism because the exact diagnostic expected of a collective tensor mode moves in the wrong direction.

8 What is not ruled out

The negative result does not rule out:

- other QATNU/SRQID Hamiltonians;
- source terms that couple to an actually collective tensor channel;
- larger 3D graph families with better continuum scaling;
- a model where the bond ladder is converged and the connected covariance is positive before hardware submission;
- a future hardware protocol using shorter circuits, layout control, mitigation, and source-off subtraction.

It does, however, set a higher bar. The next candidate should pass QMC first. The minimum gate is:

$$\chi_T^{\mathrm{conn}}/|E| > 0 \quad \text{and growing with system size at fixed local occupation,} \tag{21}$$

with stability under $\chi_{\max}$ and β before any hardware response is treated as physically meaningful.

9 Reproducibility

The relevant artifacts are contained under `hardware/phase0_qpu/`. The main result files are:

- `results/phase2_kingston_2026-05-30_summary.md`

- `results/phase2_optimization_qmc_triage.md`
- `results/qmc_full/phase2d_bond_coupled_connected_chi10_beta2.json`
- `results/qmc_full/phase2d_bond_coupled_connected_chi10_beta2_summary.md`
- `qmc_full/cube3d.py`
- `qmc_full/phase2d_bond_coupled_scan.py`
- `qmc_full/summarize_phase2d_qmc.py`

The final QMC diagnostic was generated with:

```
.venv/bin/python hardware/phase0_qpu/qmc_full/phase2d_bond_coupled_scan.py \
  --dims 2x2x2,3x3x3 \
  --couplings 0.0,0.02 \
  --seeds 1,2,3,4,5,6,7,8 \
  --chi 10 \
  --beta 2.0 \
  --slices 12 \
  --n-therm 30 \
  --n-meas 240 \
  --out ../results/qmc_full/phase2d_bond_coupled_connected_chi10_beta2.json
```

The test suite for the hardware/QMC package passes with:

```
.venv/bin/python -m pytest tests/test_phase0_qpu.py -q
```

10 Conclusion

This work should be treated as a clean negative result. The QATNU/SRQID hardware path exists, runs on IBM Quantum, and produces scalar and bond observables on graph families up to 25 qubits. The full-ladder QMC path also exists and can separate total tensor variance from connected inter-edge tensor covariance.

That separation is what ends the current branch as a spin-2 evidence path. The best-looking $K_{\mathrm{bb}} = 0.02$ candidate does not create a positive connected inter-edge tensor mode. It creates local bond-ladder variance. Future work should preserve this result, stop scaling this mechanism as a physics claim, and only return to hardware once a QMC candidate shows positive connected tensor covariance with finite-size and truncation stability.